Supplementary Table 1. Healthy Synovial Donor Information.

Cohort 1:							
Donor	**Sex**	**Age**	**BMI**	**Weight category**	**Collins Grade of cartilage**	**Time to tissue collection**	**Glucocorticoid usage** NR= none reported
1	Male	51	Average: 26.9, standard deviation: 4.7	Overweight	N/A	15.8hrs	Home: NR Hospital: NR
2	Male	28		Lean	N/A	14.8hrs	Home: NR Hospital: NR
3	Male	29		Overweight	N/A	3hrs	Home: NR Hospital: NR
4	Female	41		Overweight	N/A	7.7hrs	Home: NR Hospital: NR
5	Male	54		Lean	N/A	12.5hrs	Home: NR Hospital: NR
6	Male	59		Obese	N/A	N/A	Home: NR Hospital: NR
7	Female	56		Obese	1	N/A	Home: NR Hospital: NR
8	Female	58		Lean	2	N/A	Home: NR Hospital: NR
9	Female	50		Obese	0	N/A	Home: NR Hospital: NR
10	Female	65		Lean	1	N/A	Home: NR Hospital: NR
Cohort 2:							
11	Female	60	Average: 28.5, standard deviation: 8.6.	Obese	N/A	12 hrs	Home: prednisone; hospital: NR
12	Female	69		Lean	N/A	17hrs	Home: NR; Hospital: Prednisone
13	Male	72		Lean	N/A	21hrs	Home: budesonide, prednisone; Hospital: Prednisone
14	Male	67		Obese	N/A	24hrs	Home: NR; Hospital: Hydrocortisone injection
15	Female	60		Overweight	N/A	N/A	Home: prednisone, Hospital; Hydrocortisone injection
16	Male	41		Lean	N/A	6hrs	Home: NR Hospital; Methylprednisolone

Supplementary Table 2. Adipose donor Information. *****_Note that MUO = metabolically unhealthy. When less than 3 MUO events are logged the patient is considered metabolically healthy obese "MHO" based on bloodwork and clinical manifestations (red highlight)._

Patient	Sex	Age	Weight (kg)	BMI	Weight category	Group	MUO * Events ≥3 = MUO	Blood Glucose (fasted)	**Fasted Triglycerides**	HDL Chol.	**Co-morbidities: (Red Highlight = MUO Event)**
P11	M	40	Average: 164.8 St dev: 39.3	Average: 56.56 St dev: 9.3	Obese	MHO	0	Average: 5.04 St dev: 0.49	Average: 1.28 St dev: 0.24	Average: 1.23 St dev: 0.26	1 patient had an MUO (hypertension)
P10	M	50			Obese	MHO	1				
P49	F	57			Obese	MHO	0				
P08	F	32			Obese	MHO	0				
P50	F	37			Obese	MHO	1				

Supplementary Table 3. Statistical information, p-values.

Figure Number:	p-values:
2e	*APOD*+ cluster: Healthy vs OA p<0.0001, Healthy vs RA p<0.0001, Healthy vs REM p=0.2637. *PLIN2*+ cluster: Healthy vs OA p<0.0001, Healthy vs RA p<0.0001, Healthy v REM p=0.0717. *CXCL12*+ cluster: F=6.769, Healthy vs OA p= 0.0056, Healthy vs RA p=0.003, Healthy vs REM p=0.5072.
3a	*APOD*: p=0.0002, *NNMT*: p<0.0001, *CEBPD*: p=0.0026
3b	*APOD*: p=0.0046, *NNMT*: p=0.0116, *CEBPD*: p=0.0066
3c	*APOD*: Ctl vs. ACM P<0.0001, Ctl vs. Organic p=0.032, Ctl vs. Inter- phase p=0.7546, Ctl vs. Aqueous p=0.8512; *NNMT*: Ctl vs. ACM p<0.0001, Ctl vs. Organic p=0.0039, Ctl vs. Inter-phase p=0.8746, Ctl vs. Aqueous p= 0.0487; *CEBPD*: Ctl vs. ACM p=0.0088, Ctl vs. Organic p=0.4583, Ctl vs. Inter- phase p=0.9967, Ctl vs. Aqueous p=0.1838.
3d	*APOD*: Ctl vs. ACM p=0.2206, Ctl vs. CHCL3 p=0.9868, Ctl vs. Acetone p=0.0085, Ctl vs. Methanol p=0.7568, Ctl vs. H2O p=0.9805; *NNMT*: Ctl vs. ACM p=0.7741, Ctl vs. CHCL3 p=0.9607, Ctl vs. Acetone p=0.0034, Ctl vs. Methanol p=0.9996, Ctl vs. H2O p=0.9997; *CEBPD*: Ctl vs. ACM p=0.0101, Ctl vs. CHCL3 p=0.9792, Ctl vs. Acetone p=0.0014, Ctl vs. Methanol p=0.9997, Ctl vs. H2O p=0.9921.
4a	*APOD*: Basal vs. Differentiation media p=0.0002, Basal vs. ACM p<0.0001, Basal vs. -Dexamethasone p=0.9778, Basal vs. -Indomethacin p=0.0204, Basal vs. -Insulin p=0.0367, Basal vs. -IBMX p=0.0283; *NNMT*: Basal vs. Differentiation media p=0.1722, Basal vs. ACM p=0.0013, Basal vs. -Dexamethasone p=0.9997, Basal vs. -Indomethacin p=0.3975, Basal vs. -Insulin p=0.2896, Basal vs. -IBMX p=0.9999; *CEBPD*: Basal vs. Differentiation media p=0.5578, Basal vs. ACM p=0.0015, Basal vs. -Dexamethasone p=0.7883, Basal vs. -Indomethacin p=0.2181, Basal vs. -Insulin p=0.0367, Basal vs. -IBMX p=0.9975.
4c	*APOD*: Basal vs. FCM p<0.0001, Basal vs. Organic p=0.0038, Basal vs. Chlor p>0.9999, Basal vs. Acet p=0.5766, Basal vs. Meth p=0.698, Basal vs. H2O p=0.9985; *NNMT*: Basal vs. FCM p=0.0099, Basal vs. Organic p=0.01, Basal vs. Chlor p=0.5769, Basal vs. Acet p=0.0468, Basal vs. Meth p=0.1506, Basal vs. H2O p=0.9961; *CEBPD*: Basal vs. FCM p=0.23, Basal vs. Organic p=0.0029, Basal vs. Chlor p=0.9881, Basal vs. Acet p=0.1802, Basal vs. Meth p=0.8879, Basal vs. H2O p=0.9997.
4f	*APOD*: p=0.0089; *NNMT*: p=0.0335; *CEBPD*: p=0.0007.
4g	*APOD*: NTC vs. NTC+ FCM p<0.0001, GCR KO vs. GCR KO+ FCM p=0.0012, NTC vs. GCR KO p=0.996, NTC+ FCM vs. GCR KO+ FCM p<0.0001; *NNMT*: NTC vs. NTC+ FCM p<0.0001, GCR KO vs. GCR KO+ FCM p=0.9961, NTC vs. GCR KO p<0.0001, NTC+ FCM vs. GCR KO+ FCM p=0.0139; *CEBPD*: NTC vs. NTC+ FCM p<0.0001, GCR KO vs. GCR KO+ FCM p>0.9999, NTC vs. GCR KO p<0.0001, NTC+ FCM vs. GCR KO+ FCM p<0.0001.
4i	Cortisol score: Healthy vs OA p= 0.0026, Healthy vs RA p<0.0001, Healthy vs REM p>0.9999, OA vs RA p>0.9999, OA vs REM p>0.9999, RA vs REM p= 0.5001. FCM score: Healthy vs OA p= 0.0576, Healthy vs RA p<0.0001, Healthy vs REM p= 0.0769, OA vs RA p>0.9999, OA vs REM p>0.9999, RA vs REM p>0.9999. FCM+ GCR ant score: Healthy vs OA p>0.9999, Healthy vs RA p= 0.0024, Healthy vs REM p= 0.4651, OA vs RA p= 0.0740, OA vs REM p>0.9999, RA vs REM p>0.9999.
5a	p= 0.0015.
5b	*Adipoq*: p= 0.0088, *Hsd11b1*: p= 0.0220, *Pparg*: p= 0.0546, *Cebpd*: p= 0.0559, *Plin2*: p= 0.0187, *Cidec*: p= 0.0442.

5c	*Nr3c1*: p=0.0481, *Apod*: p=0.0416, *Cebpd*: p=0.0042, *Mt1*: p=0.0136.
5d	p=0.0082.
5e	AUC knees: GT ctl PBS vs GT ctl mBSA p<0.0001, Pdgfra-CreER;Nr3c1fl/fl PBS vs Pdgfra-CreER;Nr3c1fl/fl mBSA p<0.0001, GT ctl PBS vs Pdgfra-CreER;Nr3c1fl/fl PBS p=0.9738, GT ctl mBSA vs Pdgfra-CreER;Nr3c1fl/fl mBSA p=0.0063.
5f	CD45+ cells: GT ctl PBS vs GT ctl mBSA p=0.0048, Pdgfra-CreER;Nr3c1fl/fl PBS vs Pdgfra-CreER;Nr3c1fl/fl mBSA p<0.0001, GT ctl PBS vs Pdgfra-CreER;Nr3c1fl/fl PBS p=0.9519, GT ctl mBSA vs Pdgfra-CreER;Nr3c1fl/fl mBSA p=0.0020. CD4+ T cells: GT ctl PBS vs GT ctl mBSA p=0.0082, Pdgfra-CreER;Nr3c1fl/fl PBS vs Pdgfra-CreER;Nr3c1fl/fl mBSA p<0.0001, GT ctl PBS vs Pdgfra-CreER;Nr3c1fl/fl PBS p=0.9467, GT ctl mBSA vs Pdgfra-CreER;Nr3c1fl/fl mBSA p=0.0182.
6b	Cortisol score p-values: DDP4 vs CEBPD: p= 0.0009, DDP4 vs FABP4: p= 0.0024, DDP4 vs PPARG: p= 0.3089, CEBPD vs FABP4: p= >0.9999, CEBPD vs PPARG: p= 0.5819, FABP4 vs PPARG: p= 0.9508. FCM score p values: DDP4 vs CEBPD: p<0.0001, DDP4 vs FABP4: p= 0.0723, DDP4 vs PPARG: p= 0.4833, CEBPD vs FABP4: p= 0.1577, CEBPD vs PPARG: p= 0.0361, FABP4 vs PPARG: p>0.9999. FCM+ GCR antagonist score p-values: DDP4 vs CEBPD: p= 0.0006, DDP4 vs FABP4: p> 0.9999, DDP4 vs PPARG: p> 0.9999, CEBPD vs FABP4: p= 0.0295, CEBPD vs PPARG: p= 0.0085, FABP4 vs PPARG: p>0.9999. TGFB score p-values: DDP4 vs CEBPD: p> 0.9999, DDP4 vs FABP4: p= 0.0031, DDP4 vs PPARG: p= 0.1774, CEBPD vs FABP4: p= 0.0111, CEBPD vs PPARG: p= 0.3978, FABP4 vs PPARG: p> 0.9999.
6c	*DPP4*+ progenitors: Healthy vs OA p-value= 0.6917, Healthy vs RA p-value= 0.3918, Healthy vs REM p-value= 0.4229, OA vs RA p-value= 0.9953, OA vs REM p-value= 0.1190, RA vs REM p-value= 0.0543, *CEBPD*+ PreAd: Healthy vs OA p-value= 0.844, Healthy vs RA p-value= 0.1273, Healthy vs REM p-value= 0.8367, OA vs RA p-value= 0.6353, OA vs REM p-value= 0.5112, RA vs REM p-value= 0.1195, *FABP4*+ PreAd: Healthy vs OA p-value= 0.1307, Healthy vs RA p-value= 0.2790, Healthy vs REM p-value= 0.1033, OA vs RA p-value= 0.8106, OA vs REM p-value= 0.0021, RA vs REM p-value= 0.0039, *VIT*+Areg: Healthy vs OA p-value= 0.9493, Healthy vs RA p-value= 0.0621, Healthy vs REM p-value= 0.9136, OA vs RA p-value= 0.2663, OA vs REM p-value= 0.9926, RA vs REM p-value= 0.8179.
7a	Basal vs TNF p-value= 0.0208, Basal vs TNF+FCM p-value= 0.9796, Basal vs TNF+cortisol p-value= 0.9999, TNF vs TNF+FCM p-value= 0.0353, TNF vs TNF+cortisol p-value= 0.0228, TNF+FCM vs TNF+cortisol p-value= 0.9882.
7b	FLS vs TGFB p-value= 0.0149, FLS vs TGFB+cortisol p-value= 0.9630, TGFB vs TGFB+cortisol p-value= 0.0030.
7c	*APOD*: Cortisol vs Basal p< 0.0001, Cortisol vs Cortisol+TNFa p= 0.0086, Cortisol vs Cortisol +TGFB p<0.0001, Cortisol vs Cortisol+IL17 p= 0.9875, Cortisol vs Cortisol+ IL1B p= 0.9863, Cortisol vs Cortisol+IFNy p<0.0001, Cortisol vs Cortisol +TNFa+IFNy p<0.0001, Cortisol vs Cortisol+TNFa+IL17 p<0.0001; *CEBPD*: Cortisol vs Basal p< 0.0001, Cortisol vs Cortisol+TNFa p>0.9999, Cortisol vs Cortisol +TGFB p< 0.0001, Cortisol vs Cortisol+IL17 p= 0.0183, Cortisol vs Cortisol+ IL1B p= 0.9834, Cortisol vs Cortisol+IFNy p= 0.9920, Cortisol vs Cortisol +TNFa+IFNy p= 0.3960, Cortisol vs Cortisol+TNFa+IL17 p= 0.9994; *PLIN2*: Cortisol vs Basal p= 0.0091, Cortisol vs Cortisol+TNFa p= 0.0771, Cortisol vs Cortisol +TGFB p< 0.0001, Cortisol vs Cortisol+IL17 p= 0.0445, Cortisol vs Cortisol+ IL1B p= 0.0035, Cortisol vs Cortisol+IFNy p< 0.0001, Cortisol vs Cortisol +TNFa+IFNy p< 0.0001, Cortisol vs Cortisol+TNFa+IL17 p= 0.3853.

7d	*ADIPOQ*: Basal vs GCR ant p> 0.9999, Basal vs ADM p= 0.0124, Basal vs ADM+GCR ant p> 0.9999, GCR ant vs ADM p= 0.0124, GCR ant vs ADM+ GCR ant p> 0.9999, ADM vs ADM+ GCR ant p= 0.0124; *FABP4*: Basal vs GCR ant p> 0.9999, Basal vs ADM p< 0.0001, Basal vs ADM+GCR ant p> 0.9999, GCR ant vs ADM p< 0.0001, GCR ant vs ADM+ GCR ant p> 0.9999, ADM vs ADM+ GCR ant p< 0.0001, *LEPTIN*: Basal vs GCR ant p= 0.9987, Basal vs ADM p= 0.0034, Basal vs ADM+GCR ant p= 0.5026, GCR ant vs ADM p= 0.0040, GCR ant vs ADM+ GCR ant p= 0.5830, ADM vs ADM+ GCR ant p= 0.0216; *PPARG*: Basal vs GCR ant p= 0.9187, Basal vs ADM p= 0.0001, Basal vs ADM+GCR ant p> 0.9999, GCR ant vs ADM p= 0.0002, GCR ant vs ADM+ GCR ant p= 0.9095, ADM vs ADM+ GCR ant p= 0.0001.
7e	FLS+ADM vs FLS p<0.0001, FLS+ADM vs FLS+ADM+TGF-B1 p<0.0001, FLS+ADM vs FLS+ADM+TNF+IFN-y p= 0.0088.

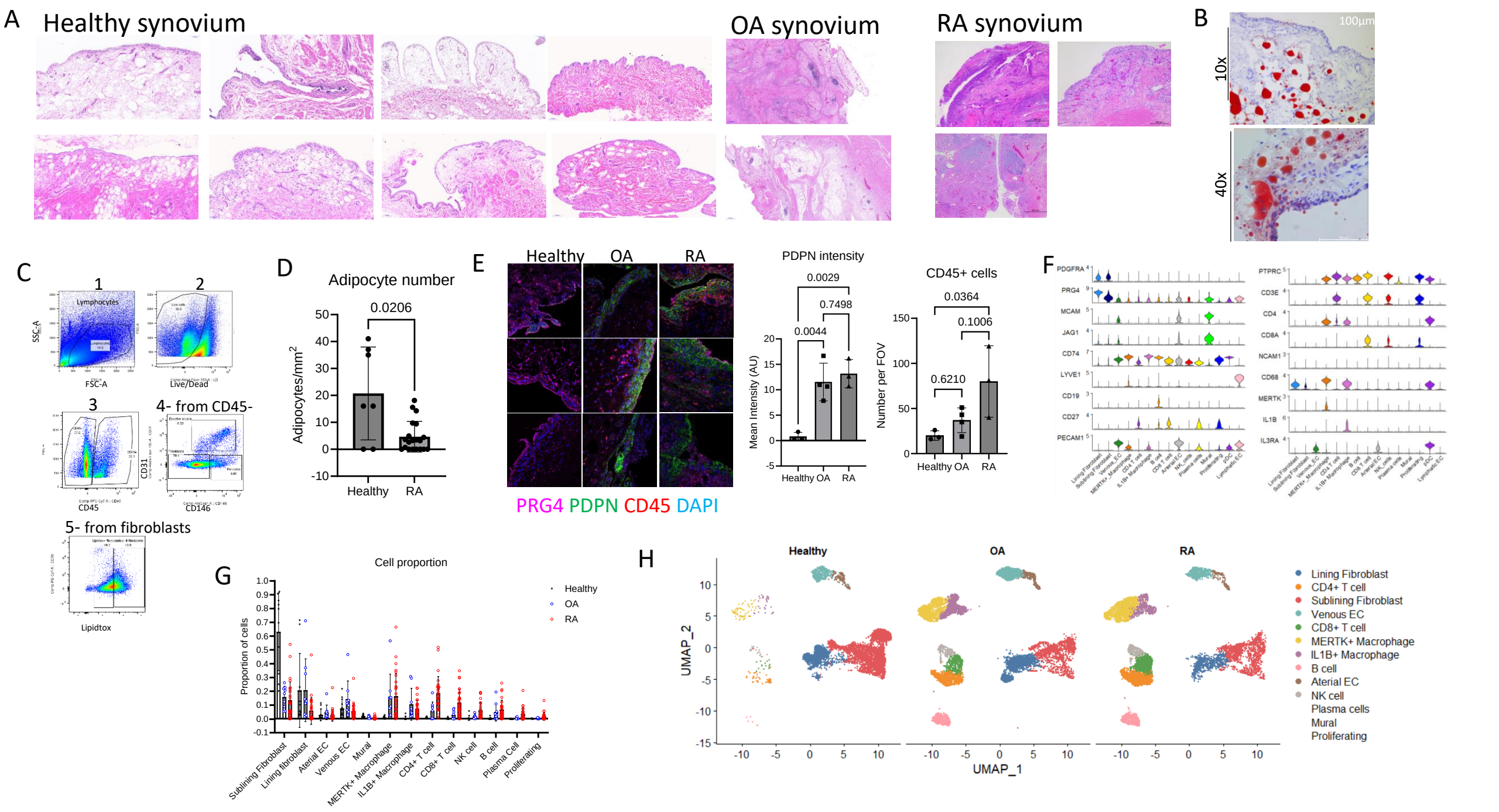

Supplementary Figure 1.

Supplementary Figure 1. A. H&E staining on paraffin embedded healthy synovial tissue sections. n=8 biological samples. B. Oil red O staining of OCT embedded healthy synovium. C. Gating strategy used to quantify fibroblasts in Figure 1b. D. Adipocyte quantification. Adipocytes were identified by morphology on H&E images of healthy and RA synovium from AMP phase 2 biopsies, healthy n=7, RA n=20. P values were calculated using a two-tailed student's T test. E. Images used for quantification in Figure 1c, n=3 biological replicates representative of one independent experiment. P values were calculated using an ordinary one-way ANOVA followed by Tukey's multiple comparison post-hoc testing. F. Major marker expression defining each cluster. G. Cell cluster proportions among healthy, OA, and naïve RA synovial cells and UMAP separated by disease state. Healthy n=10, OA n=9, RA n=28 biological samples. H. UMAP in figure 1d split by disease state. Source data are provided as a Source Data file.

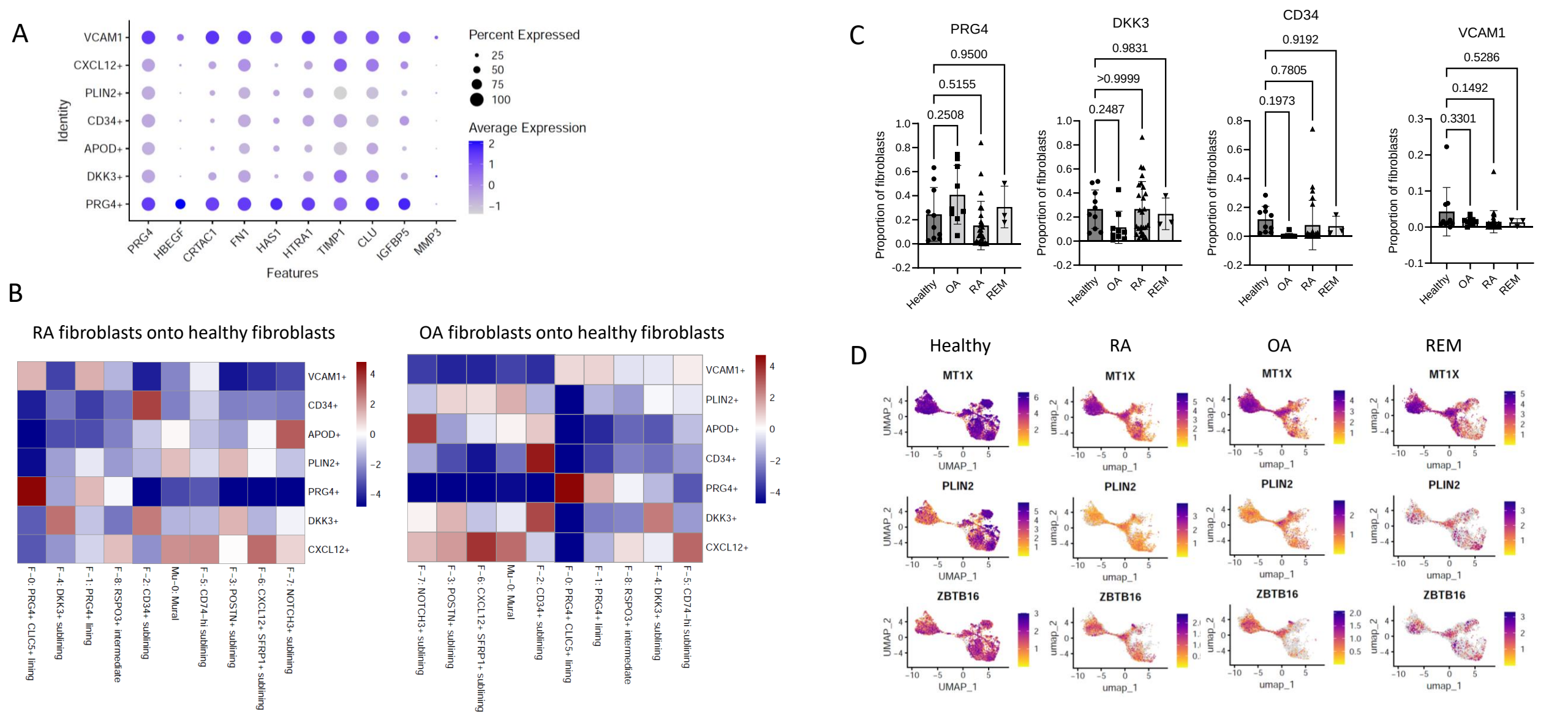

Supplementary Figure 2 S. Fig. 2. A. PRG4+ and VCAM1+ fibroblasts express high levels of lining fibroblast markers. B. Heatmaps show odds ratios for the fibroblast clusters, with rows corresponding to fibroblast clusters from healthy synovial fibroblasts and columns corresponding to fibroblast clusters from Zhang, *et al*, 2022. Blue-red color scale indicates the log(OR) for a given pair of states (OR is the ratio of odds of mapping a cluster in Zhang, *et al*, 2022 to a given healthy fibroblast cluster compared to odds of mapping other fibroblasts in Zhang, *et al*, 2022 onto the same cluster of this study), with higher values indicating greater correspondence. C. Quantification of fibroblast proportions mapping to each cluster. Df=44. PRG4: F=3.383, DKK3: F=1.410, CD34: F=1.099, VCAM1: F=1.351. Healthy n=10, OA n=9, RA n=26, REM n=3 biological samples. P values were calculated using an ordinary one-way ANOVA followed by Dunnett's multiple comparison post-hoc testing. D. Healthy fibroblasts globally upregulate genes which are involved in metabolism, including, *PLIN2*, *MT1X*, and *ZBTB16.* Source data are provided as a Source Data file.

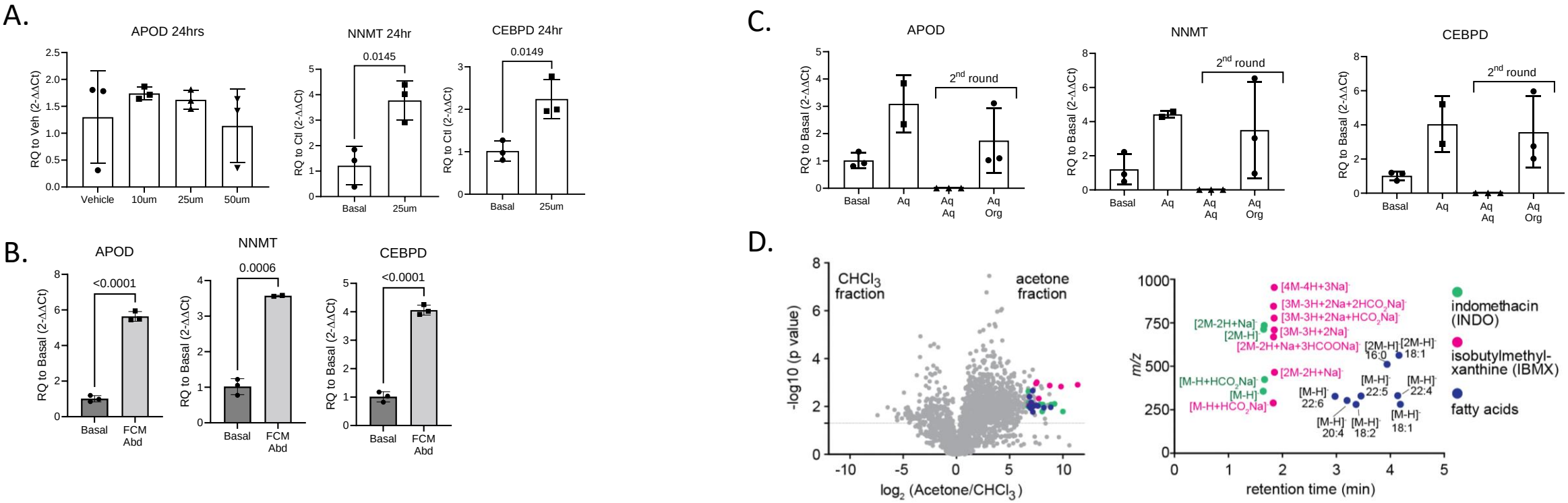

Supplementary Figure 3 A. Fibroblasts cultured with 10um oleate+10um palmitate for 24hrs do not induce APOD expression, n=3 technical replicates representative of one independent experiment. B. Abdominally derived FCM induces *APOD*, *NNMT*, and *CEBPD* expression, n=3 technical replicates representative of one independent experiment (NNMT FCM n=2). A-B: P values were calculated using a two-tailed student's T test. C. Bligh and dyer separation of adipocyte conditioned media (ACM) shows that the active molecule is in organic and aqueous fractions of ACM (Shown in Fig. 3c). Due to incomplete separation; a second round of bligh and dyer on the aqueous fraction was performed and results in all activity going to the organic fraction ("aq org"). Basal, Aq aq, Aq Org n=3, Aq n=2 technical replicates representative of one independent experiment. D. Three independently separated fractions of chloroform, acetone and methanol were normalized to the lipid weight and subject to HPLC-QToF-MS negative mode analysis. The non-stimulatory chloroform fractions were compared to the stimulatory acetone fractions by lipidomics analysis. The ions with highest fold change and intensity in the acetone fraction were selected and plot against the retention time. The fatty acid class (blue dots of seven different fatty acids), indomethacin (green dots of four alternate and multimer ion adducts), and isobutylmethylxanthine (pink dots of four alternate and multimer ion adducts) were identified. Source data are provided as a Source Data file.

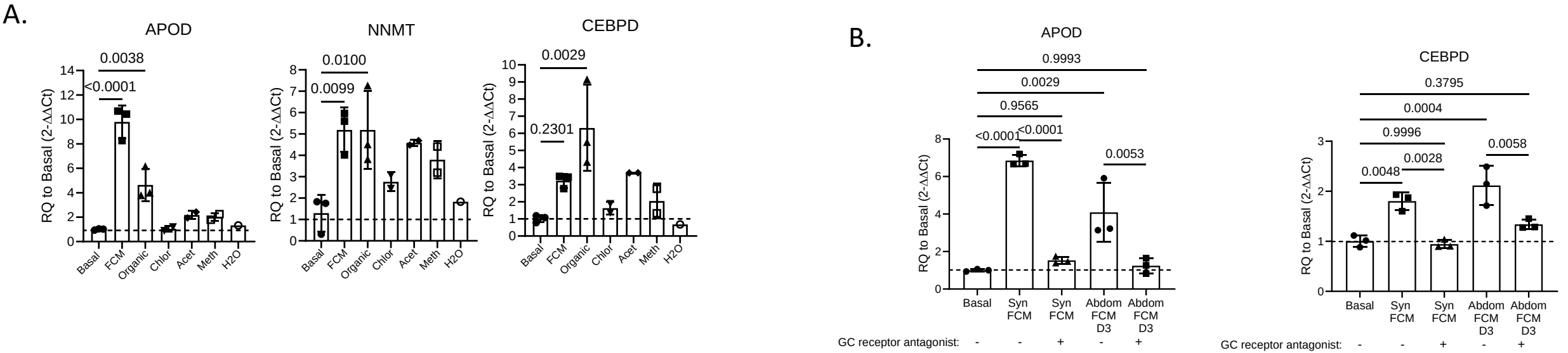

Supplementary Figure 4. A. FCM was separated using the Bligh and Dyer method into aqueous and organic phases. Then, the organic phase was taken for solid phase separation and eluted based on polarity using chloroform, acetone, methanol, and water. Testing activity of each fraction; activity was primarily in the acetone and methanol fractions of the organic phase. Basal, FCM, Organic n=3, Chlor, Acet, Meth n=2, H20 n=1 technical replicates representative of two independent experiments. P values were calculated using an ordinary one-way ANOVA followed by Dunnett's multiple comparison post-hoc testing. B. APOD and CEBPD upregulation are suppressed by the GCR antagonist mifepristone, n=3 technical replicates representative of one independent experiment. D3 stands for donor 3. P values were calculated using an ordinary one-way ANOVA. Source data are provided as a Source Data file.

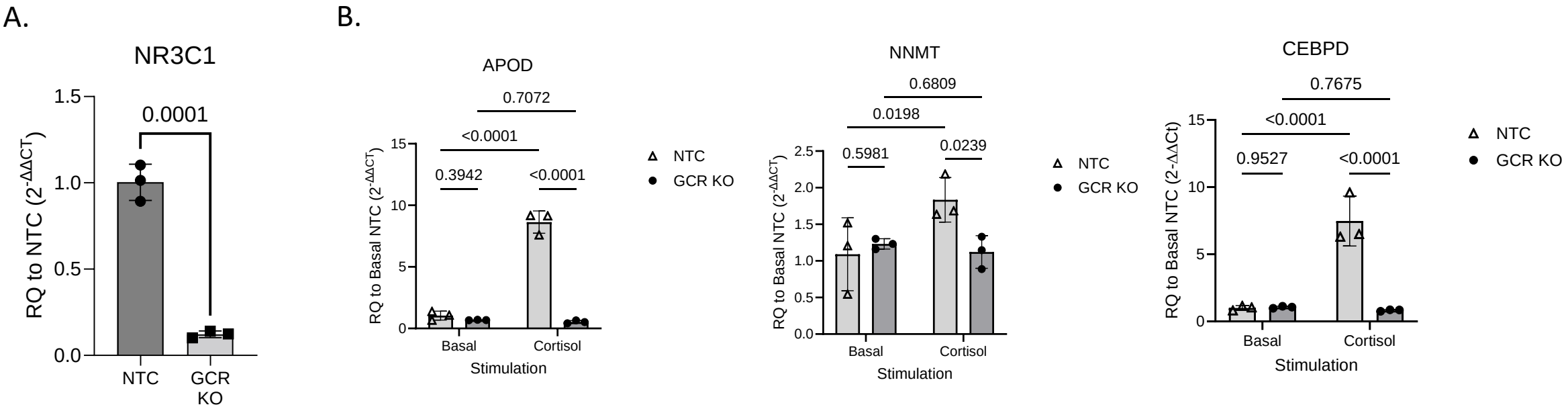

Supplementary Figure 5. A. CRISPR-Cas9 of the glucocorticoid receptor gene, *NR3C1*, results in significant reduction of *NR3C1* gene expression compared to the non-targeting control (NTC), n=3 technical replicates representative of one independent experiment. P values were calculated using a two-tailed student's T test. B. *NR3C1* knockout renders cells unresponsive to cortisol, n=3 technical replicates representative of one independent experiment. P values were calculated using a two way ANOVA with Uncorrected Fisher's LSD. Source data are provided as a Source Data file.

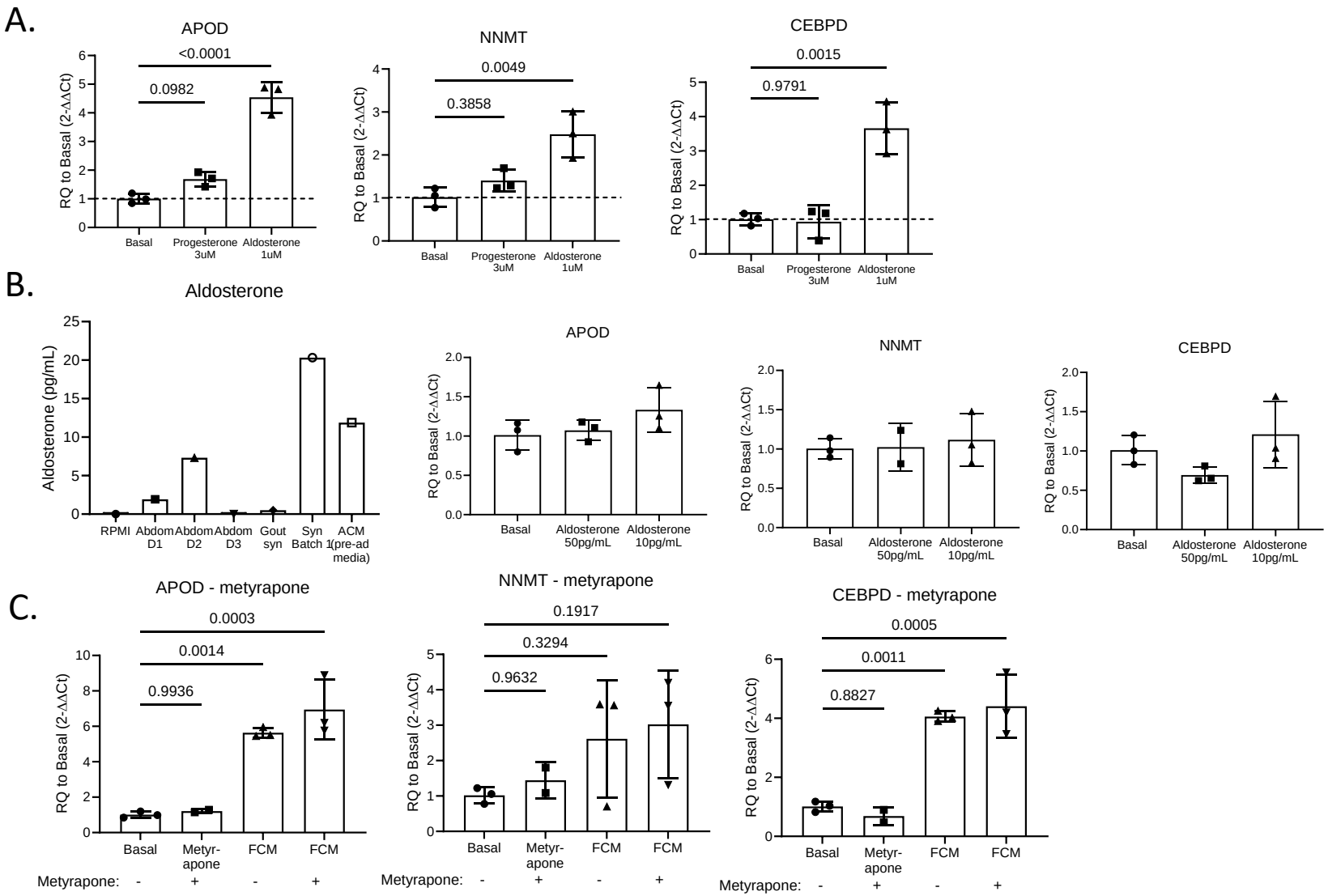

Supplementary Figure 6. A. Progesterone has no activity; aldosterone contains activity at 3µM. n=3 technical replicates representative of one independent experiment. B. Aldosterone levels in FCM as measured by ELISA; n=1 technical replicate per biological sample (6 total). Physiologically relevant levels contain no activity as measured by gene expression of APOD, NNMT, or CEBPD, n=3 technical replicates representative of one independent experiment (NNMT 50pg/mL aldosterone n=2). C. Blocking Hydroxysteroid 11-Beta Dehydrogenase 1 conversion of cortisone to cortisol with metyrapone does not block FCM activity, Basal, FCM, FCM+metyrapone n=3, Metyrapone n=2 technical replicates representative of one independent experiment. A, C: P values were calculated using an ordinary one-way ANOVA followed by Dunnett's multiple comparison post-hoc testing. Source data are provided as a Source Data file.

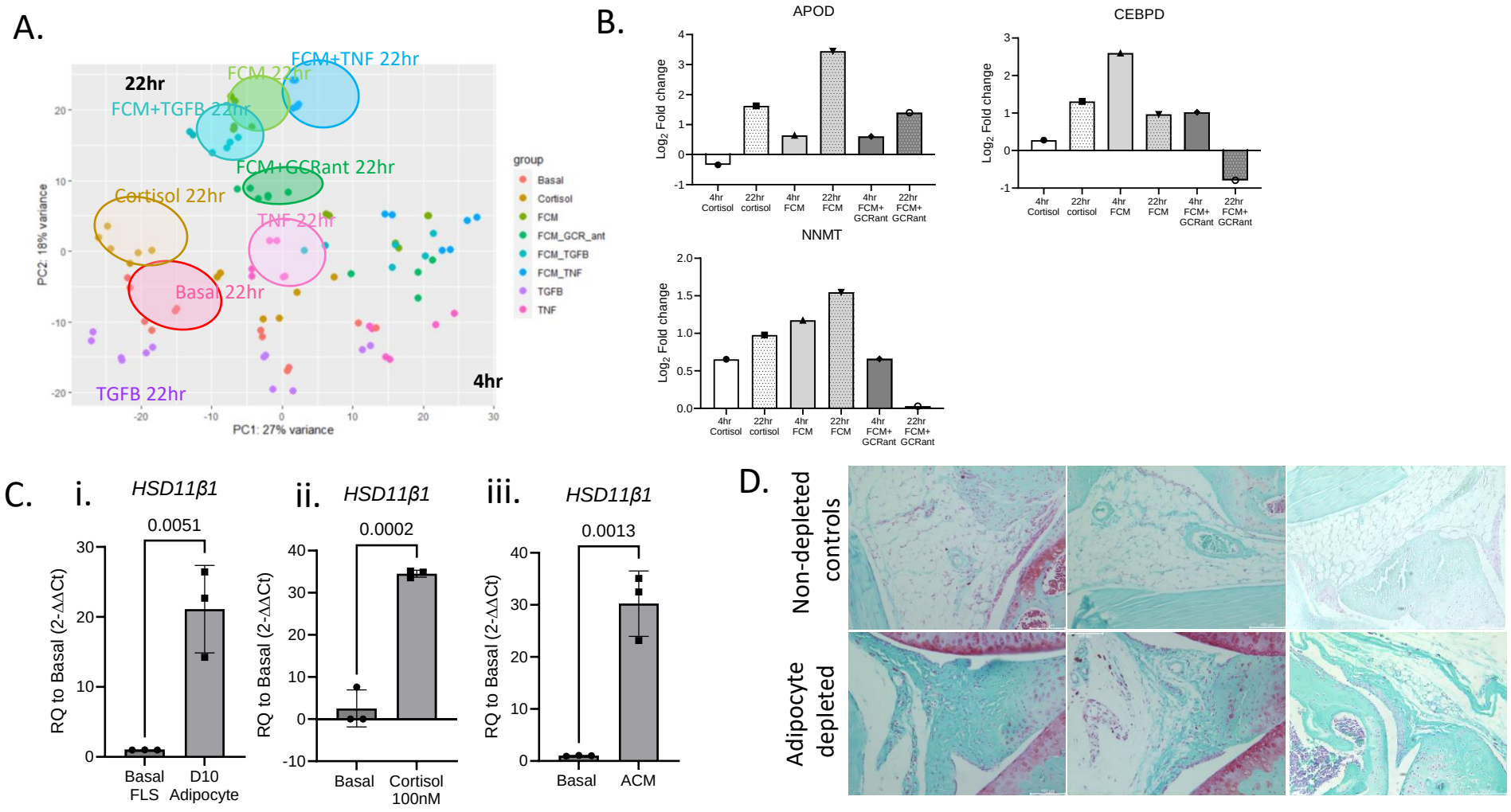

Supplementary Figure 7. A. PCA of bulk RNA sequencing samples. B. Plotting of bulk RNAseq individual gene expression of APOD, CEBPD, and NNMT. C. *HSB11B1* gene expression. i. We differentiated preadipocytes into mature adipocytes for 10 days, then isolated RNA and performed qPCR analysis for *HSD11B1*. We also isolated RNA from a cultured synovial RA fibroblast cells line and found that cultured adipocytes express *HSD11B1* at >20-fold higher levels than synovial fibroblasts. ii. We stimulated synovial fibroblasts with cortisol or iii. adipocyte conditioned media (ACM) and found that both stimulated fibroblasts substantially upregulate their expression of *HSD11B1* (~30-fold). This suggests that at baseline, adipocytes are a major source of *HSD11B1*, but expression can be induced in other cell types via cortisol and adipocyte products. n=3 technical replicates representative of one independent experiment. P values were calculated using a two-tailed student's T test. D. Source images for adipocyte quantification in figure 5a, n=3 biological replicates representative of one independent experiment. Source data are provided as a Source Data file.

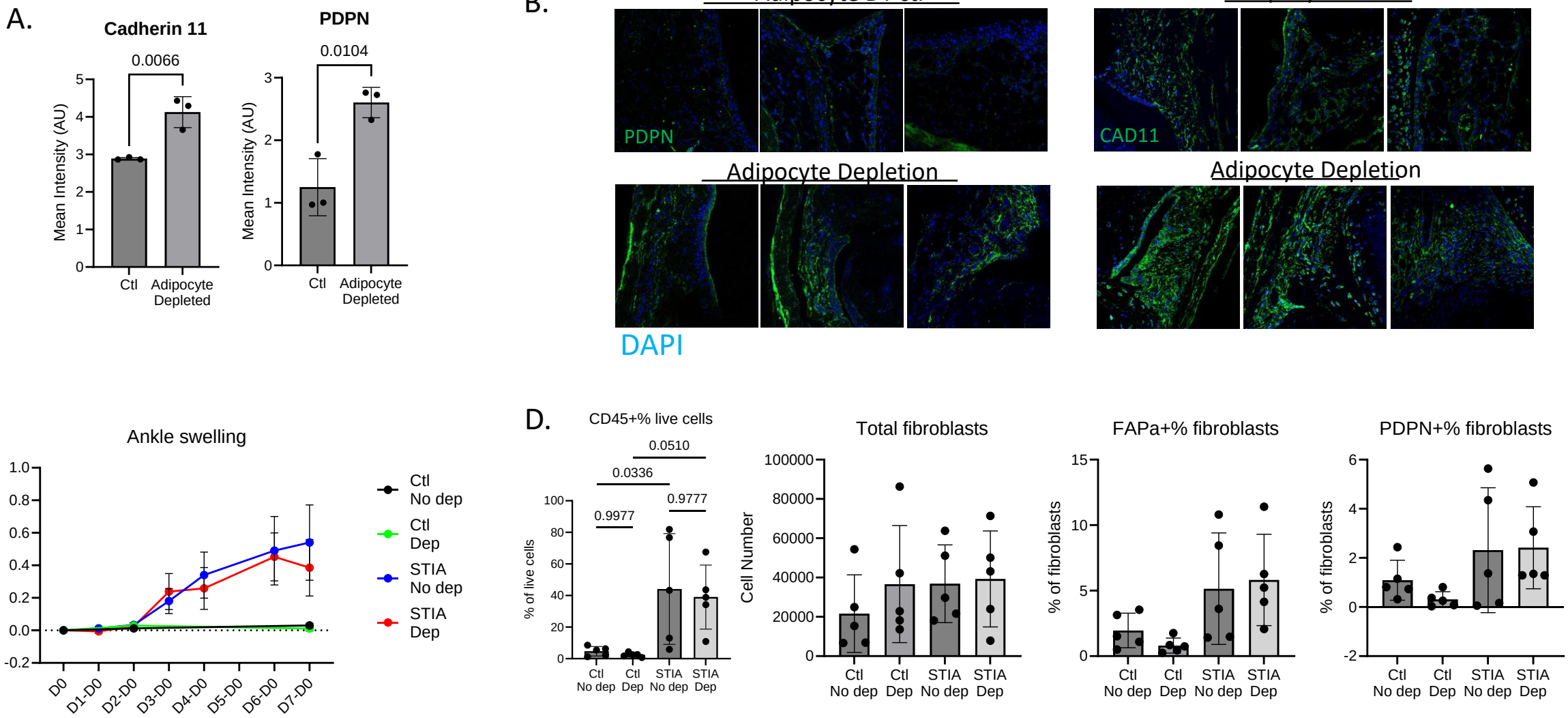

Supplementary figure 8. Adipocyte depletion in naïve mice and in the K/BxN serum transfer inflammatory arthritis (STIA) model. A. Mean fluorescence intensity of cadherin-11 and PDPN immunostaining in PDGFRA+ cells in naïve knee joints with or without 8 weeks of adipocyte depletion. Ctl= diphtheria toxin injected genotype controls, n=3 biological replicates representative of one independent experiment. P values were calculated using a two-tailed student's T test. B. Images used for quantification in D. C-D: Mouse ankles were depleted 2 weeks prior to STIA induction. C. Measures of ankle swelling by caliper, n= 10 biological replicates representative of one independent experiment. D. Flow cytometry performed on ankle synovial tissue quantifying immune cells (CD45+) and fibroblasts (CD45-, CD146-, CD31-), n= 5 biological replicates representative of one independent experiment. P values were calculated using an ordinary one-way ANOVA followed by Tukey's multiple comparison post-hoc testing. Source data are provided as a Source Data file.

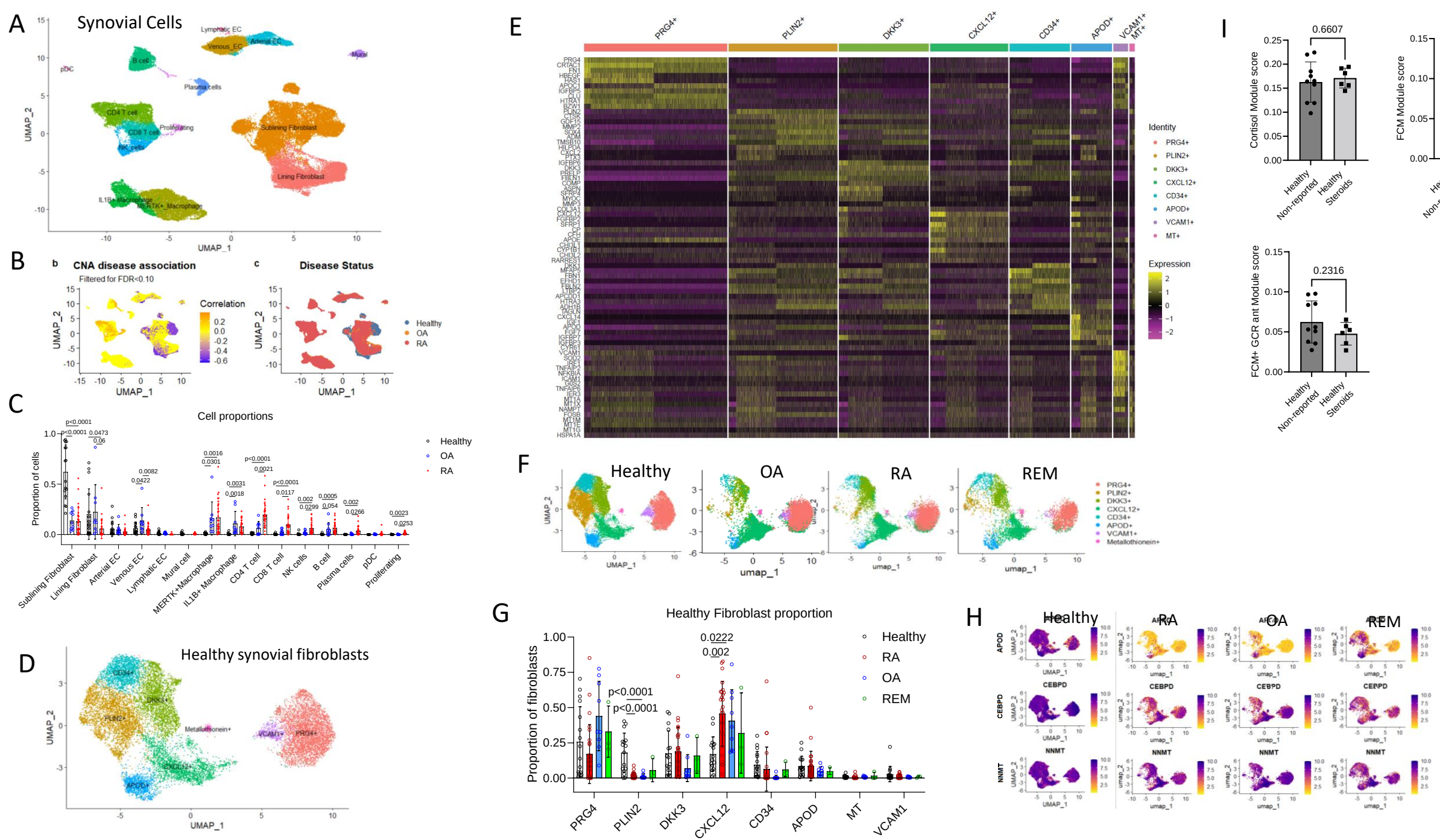

Supplementary Figure 9.

Supplementary Figure 9. Analysis of healthy steroid users and non-users. A. Synovial cells from all healthy steroid users and non-users, OA, and naïve RA donors were harmonized and clustered into a single UMAP. B. UMAP projection from (A) colored by correlation with arthritis (orange) or health (purple) using covarying neighborhood analysis (CNA). C. Cell cluster proportions among healthy, OA, and naïve RA synovial cells and UMAP separated by disease state, healthy n=10, OA n=9, RA n=28. D. Fine clustering analysis on healthy synovial fibroblasts defines 8 distinct clusters. E. Heatmap of the top 10 DEGs per cluster. F. Symphony mapping of OA, naïve RA, and remission fibroblasts to healthy synovial fibroblast reference. G. Quantification of fibroblast proportions mapping to each cluster, healthy n=10, OA n=9, RA n=26, REM n=3. H. Healthy synovium is enriched in APOD, CEBPD, and NNMT expression compared to OA and RA fibroblasts, and is partially restored in remission fibroblasts. I. Application of bulk-RNA sequencing defined module scoring to single cell pseudobulk data (reads collapsed over patient) reveals that FCM and cortisol activation is similar in fibroblasts from healthy steroid users and non-users, non-reported n=10, reported n=6. P values were calculated using a two-tailed student's T test. C, G: P values were calculated using an ordinary one-way ANOVA followed by Tukey's multiple comparison post-hoc testing. Source data are provided as a Source Data file.

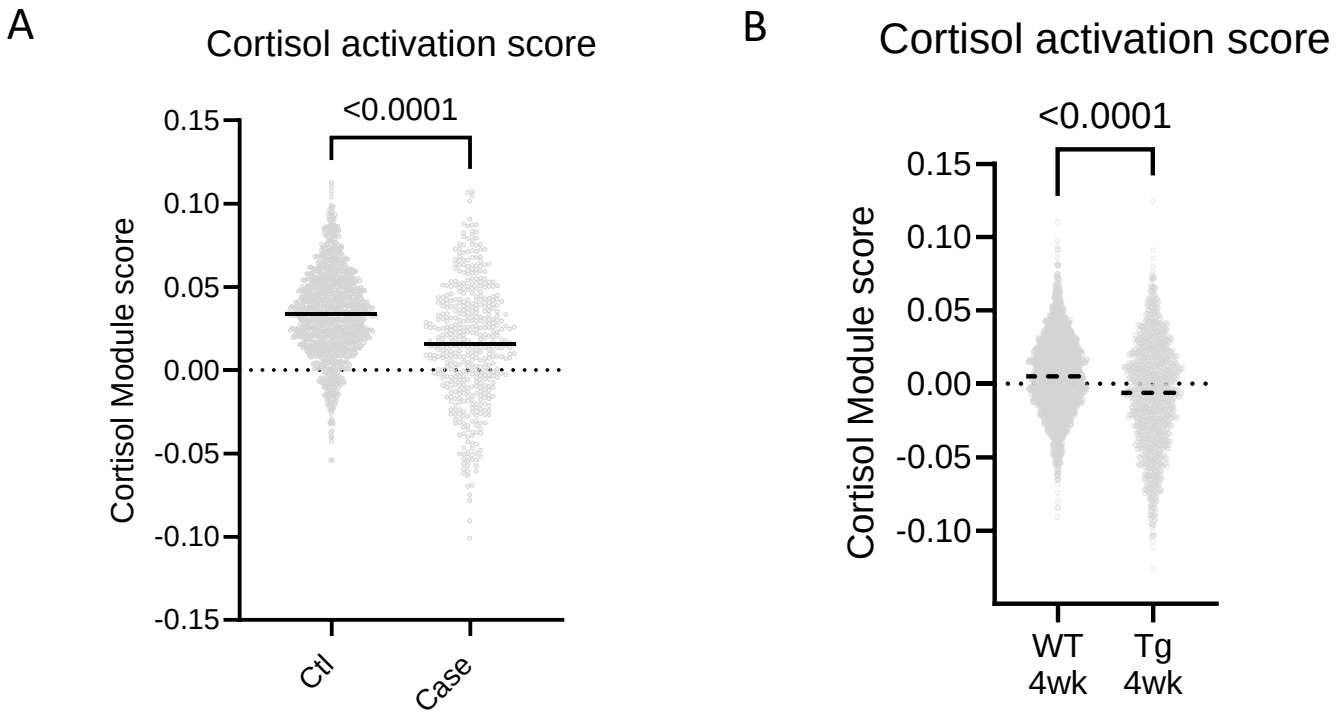

Supplementary Figure 10. A. Cortisol activation score, as defined by bulk RNA sequencing, was applied to wildtype mouse synovial sublining fibroblasts from Wei et. al.. Ctl= healthy (n=1,138 cells), case=serum transfer arthritis (n=493 cells), day 10. B. The cortisol activation score was applied to synovial fibroblasts from the Armaka et. al. WT 4wk= healthy (n=2,852 cells), Tg 4wk= hTNFtg spontaneous arthritis mice (n=1,553 cells). A-B: P values were calculated using a two-tailed student's T test. Source data are provided as a Source Data file.

A.

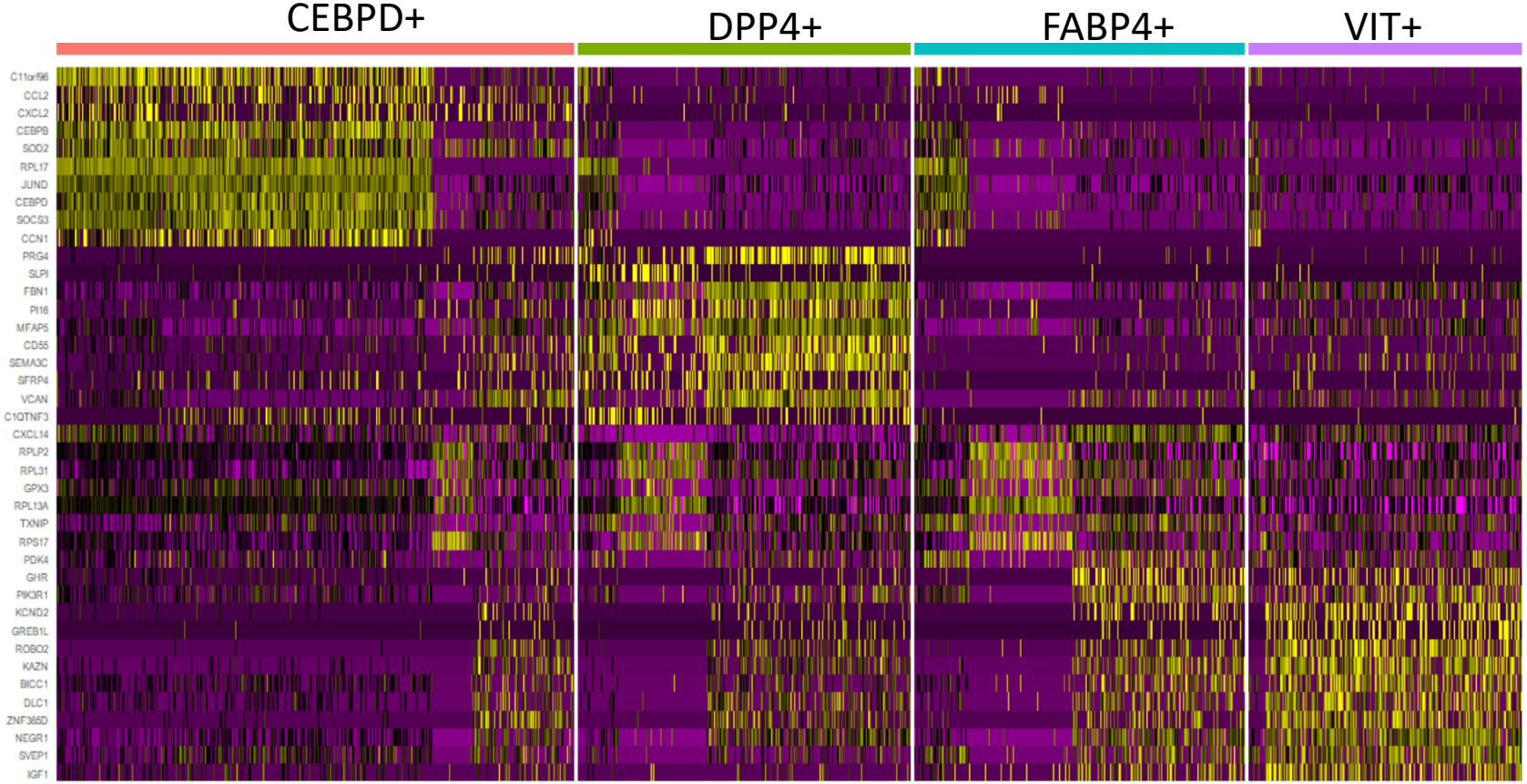

Supplementary Figure 11. A. Top ten markers of PDGFRα+ non mesothelial cells from VAT (visceral) and SAT (subcutaneous) adipose tissue.

A.

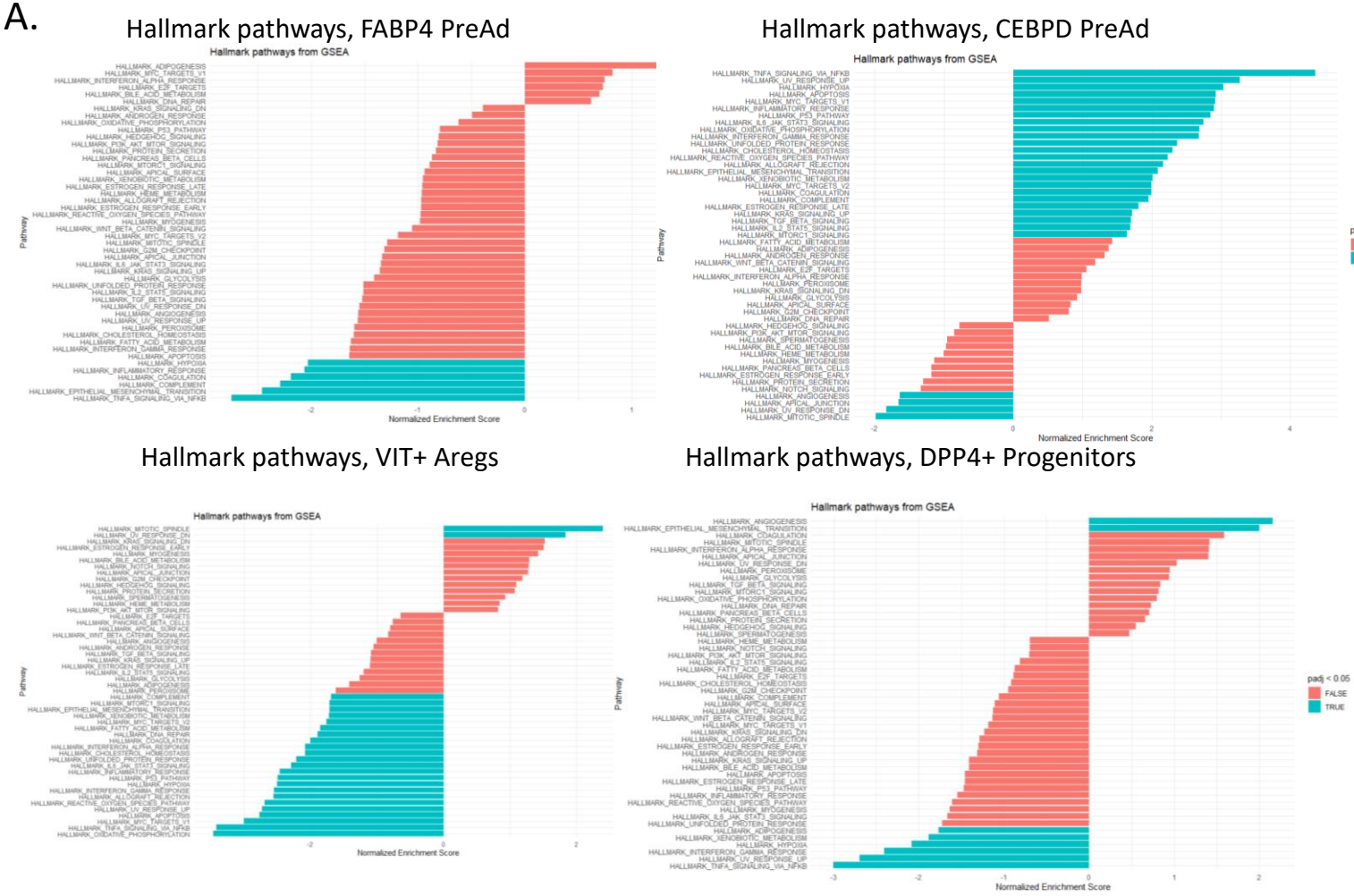

B.

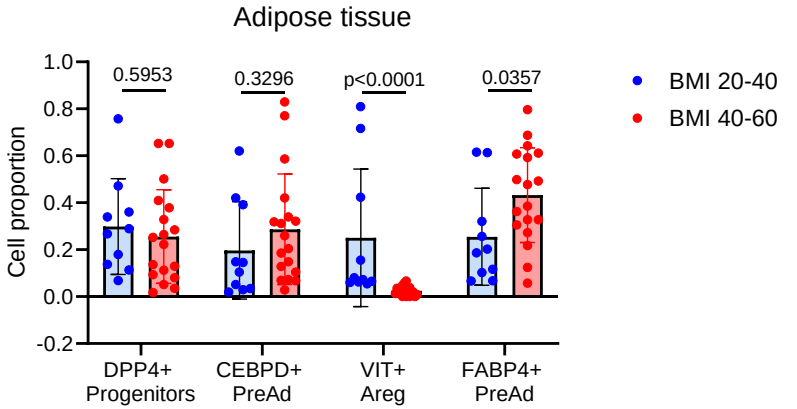

Supplementary Figure 12. A. FGSEA on adipose populations using Hallmark Pathways. B. Adipose stromal population proportions by BMI, BMI 20-40 n=10, BMI 40-60 n=18. P values were calculated using a two-tailed student's T test. Source data are provided as a Source Data file.

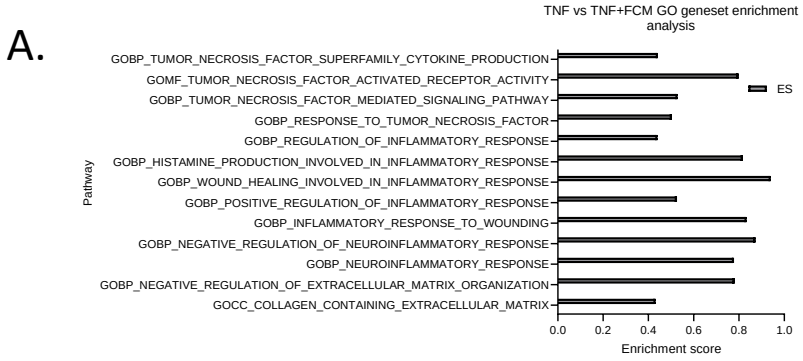

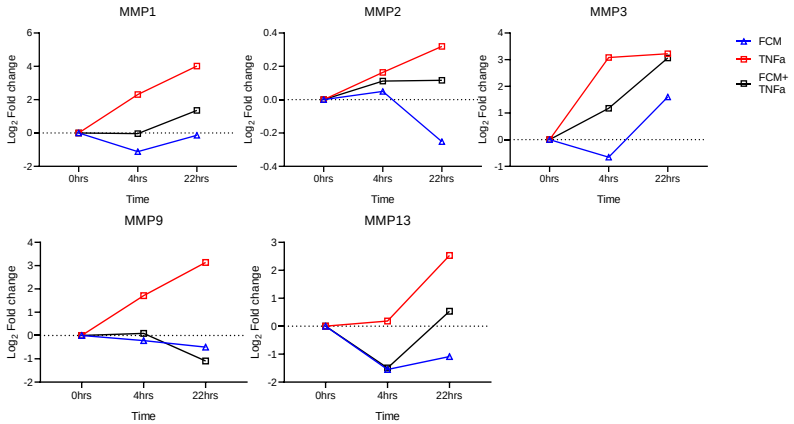

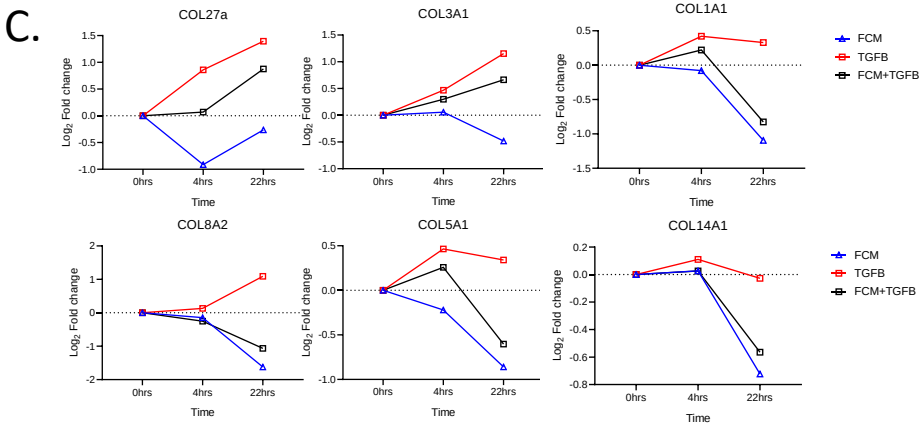

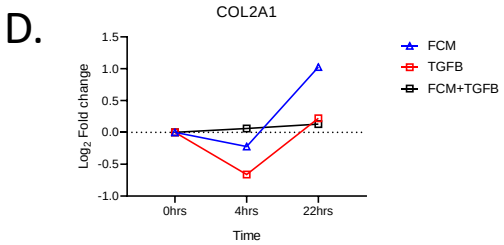

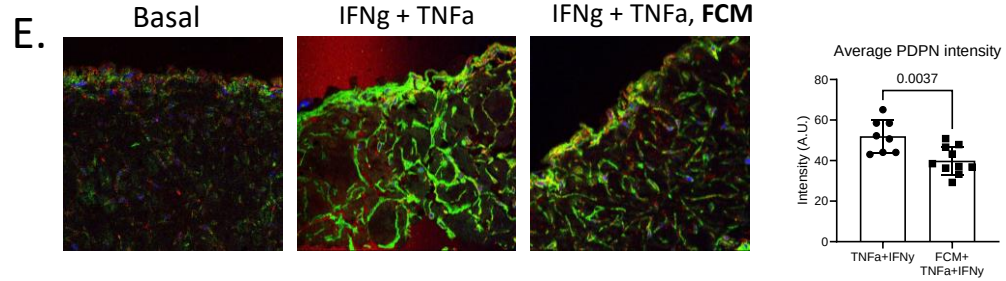

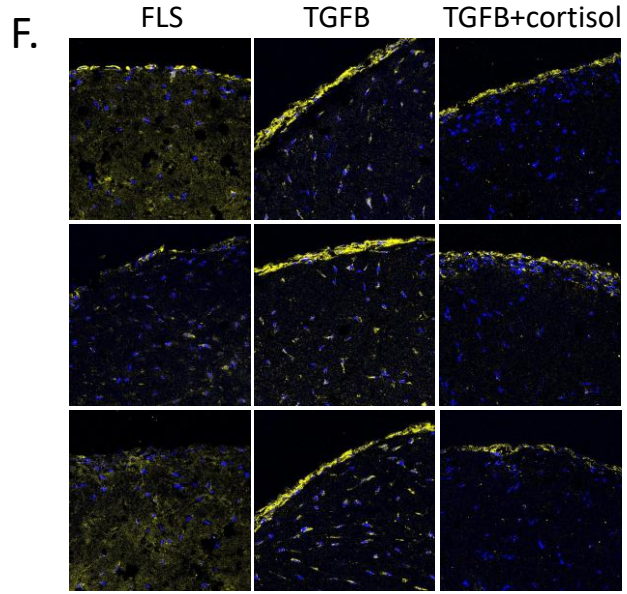

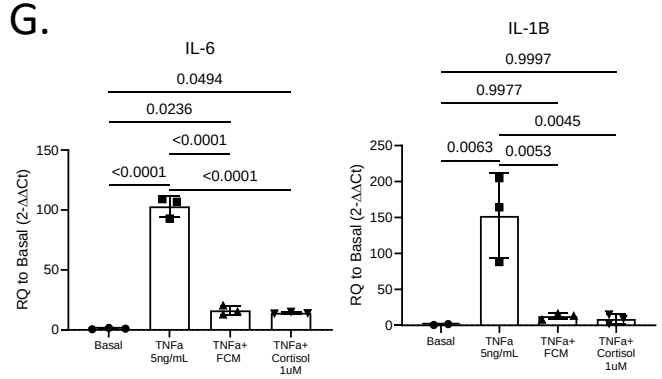

Supplementary Figure 13

Supplementary Figure 13. A. GSEA analysis using GO terms on bulk RNA sequencing data. Enriched pathways are “rescued” by FCM to basal levels. B. FCM reduces MMP upregulation by TNFa. C. FCM rescues fibrotic collagens upregulated by TGFB. D. FCM does not impact non-fibrotic collagens. E. PDPN staining of micromass sections and intensity quantification performed in ImageJ, n=4 biological replicates and 2 technical replicates (8 total replicates) representative of one independent experiment. P values were calculated using a two-tailed student’s T test. F. Cortisol (1uM) prevents TGFB (10ng/mL) induced fibrosis as measured by collagen 1a1 immunostaining (Day 21), n=3 biological replicates representative of one independent experiment. G. FCM and cortisol inhibit TNFa induced pro-inflammatory changes, n=3 technical replicates representative of one independent experiment. P values were calculated using an ordinary one-way ANOVA followed by Sidak’s multiple comparison post-hoc testing. Source data are provided as a Source Data file.

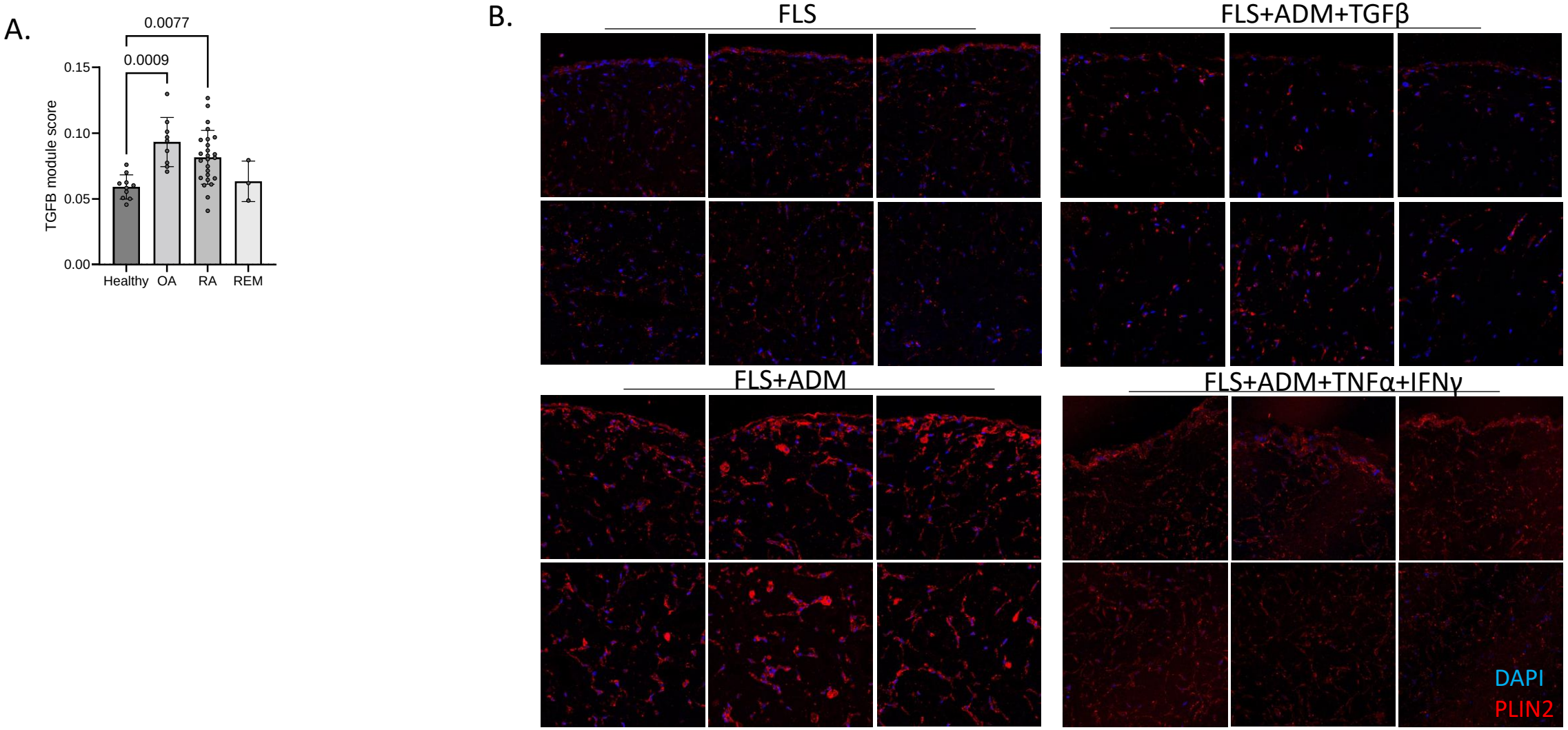

Supplementary Figure 14. A. Bulk-RNA sequencing defined TGFB activation score was applied to a pseudobulk analysis of single cell RNA sequenced synovial fibroblasts, healthy n=10, OA n=9, RA n=26, REM n=3 biological samples. P values were calculated using a Kruskal-Wallis test. B. Images used for quantification of Plin2 expression in figure 7e, n=3 biological replicates and 2 technical replicates (6 total replicates) representative of one independent experiment. Source data are provided as a Source Data file.

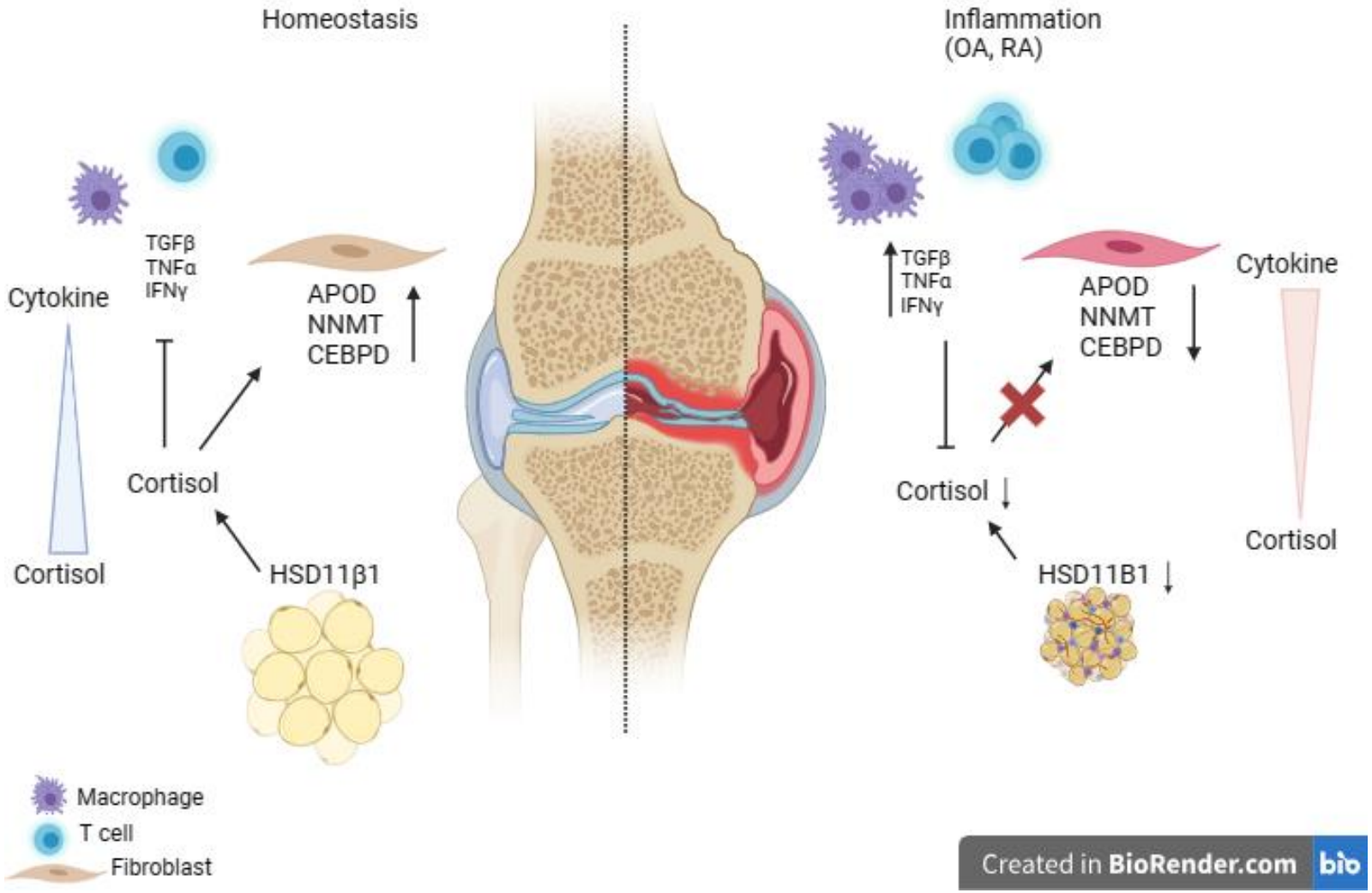

Supplementary Figure 15. A graphic summary of the findings of the paper. Supplementary figure 15 Created with BioRender.com released under a Creative Commons Attribution-NonCommercial-NoDerivs 4.0 International license (https://creativecommons.org/licenses/by-nc-nd/4.0/deed.en).

Accelerating Medicines Partnership: RA/SLE Network

Jennifer Albrecht[12], Jennifer H. Anolik[12], William Apruzzese[13], Jennifer L. Barnas[12], Joan M. Bathon[14], Ami Ben-Artzi[15], Brendan F. Boyce[12], David L. Boyle[16], S. Louis Bridges Jr.[17,18], Vivian P. Bykerk[17,18], Debbie Campbell[12], Arnold Ceponis[16], Adam Chicoine[1], Michelle Curtis[6, 2,3,9,19], Kevin D. Deane[11], Edward DiCarlo[20], Laura T. Donlin[17,18], Patrick Dunn[21,22], Andrew Filer[23,24,25], Hayley Carr[23,25], Gary S. Firestein[16], Lindsy Forbess[15], Laura Geraldino-Pardilla[14], Susan M. Goodman[17,18], Ellen M. Gravallese[1], Deepak Rao[1], Peter K. Gregersen[26], Joel M. Guthridge[27], Maria Gutierrez-Arcelus[2,3,9,19,28], V. Michael Holers[11], Diane Horowitz[26], Laura B. Hughes[29], Lionel B. Ivashkiv[17,18], Kazuyoshi Ishigaki[30], Judith A. James[27], Joyce B. Kang[1,2,3,9,19,] Gregory Keras[1], Amit Lakhanpal[17,18], James A. Lederer[10], Miles J. Lewis[31,32], Yuhong Li[1], Katherine Liao[1], Arthur M. Mandelin II[33], Ian Mantel[17,18], Kathryne E. Marks[6], Mark Maybury[23,25], Andrew McDavid[34], Mandy J. McGeachy[35], Joseph R. Mears[1, 2,3,9,19], Nida Meednu[12], Nghia Millard[6, 2,3,9,19,] Larry Moreland[11], Saba Nayar[23,24], Alessandra Nerviani[31,32], Dana E. Orange[17,39], Harris Perlman[33], Costantino Pitzalis[31,32,36], Javier Rangel-Moreno[12], Karim Raza[23,25], Yakir Reshef[1, 2,3,9,19,] Christopher Ritchlin[12], Felice Rivellese[31,32], William H. Robinson[37], Laurie Rumker[1, 2,3,9,19], Ilfita Sahbudin[23,25], Saori Sakaue[1, 2,3,9,19,] Jennifer A. Seifert[11], Dagmar Scheel-Toellner[23,25,] Anvita Singaraju[17,18], Kamil Slowikowski[1, 2,3,9,19], Melanie Smith[17], Darren Tabechian[12], Paul J. Utz[37], Kathryn Weinand[1, 2,3,9,19], Dana Weisenfeld[1], Michael H. Weisman[15], Qian Xiao[1, 2,3,9,19], Zhu Zhu[1], Zhihan J. Li[1], Andrew Cordle[38] &Aaron Wyse[38]

Affiliations:

[10]Department of Surgery, Brigham and Women's Hospital, Boston, Massachusetts, USA. [11]Division of Rheumatology, University of Colorado School of Medicine, Aurora, CO, USA. [12] Division of Allergy, Immunology and Rheumatology, Department of Medicine, University of Rochester Medical Center, Rochester, NY, USA. [13]Accelerating Medicines Partnership: RA/SLE Network, Bethesda, MD, USA. [14]Division of Rheumatology, Columbia University College of Physicians and Surgeons, New York, NY, USA. [15]Division of Rheumatology, Cedars-Sinai Medical Center, Los Angeles, CA, USA. [16]Division of Rheumatology, Allergy and Immunology, University of California, San Diego, La Jolla, CA, USA. [17]Hospital for Special Surgery, New York, NY, USA. [18]Weill Cornell Medicine, New York, NY, USA. [19]Broad Institute of MIT and Harvard, Cambridge, MA, USA. [20]Department of Pathology and Laboratory Medicine, Hospital for Special Surgery, New York, NY, USA. [21]Division of Allergy, Immunology and Transplantation, National Institute of Allergy and Infectious Diseases, National Institutes of Health, Bethesda, MD, USA. [22]Northrop Grumman Health Solutions, Rockville, MD, USA. [23]Rheumatology Research Group, Institute for Inflammation and Ageing, University of Birmingham, Birmingham, UK. [24]Birmingham Tissue Analytics, Institute of Translational Medicine, University of Birmingham, Birmingham, UK. [25]NIHR Birmingham Biomedical Research Center and Clinical Research Facility, University of Birmingham, Queen Elizabeth Hospital, Birmingham, UK. [26]Feinstein Institute for Medical Research, Northwell Health, Manhasset, New York, NY, USA. [27]Department of Arthritis and Clinical Immunology, Oklahoma Medical Research Foundation, Oklahoma City, OK, USA, [28]Division of Immunology, Department of Pediatrics, Boston Children's Hospital and Harvard Medical School, Boston, MA, USA. [29]Division of Clinical Immunology and Rheumatology, Department of Medicine,

University of Alabama at Birmingham, Birmingham, AL, USA. [30]Laboratory for Human Immunogenetics, RIKEN Center for Integrative Medical Sciences, Yokohama, Japan. [31]Centre for Experimental Medicine and Rheumatology, EULAR Centre of Excellence, William Harvey Research Institute, Queen Mary University of London, London, UK. [32]Barts Health NHS Trust, Barts Biomedical Research Centre (BRC), National Institute for Health and Care Research (NIHR), London, UK. [33]Division of Rheumatology, Department of Medicine, The Feinberg School of Medicine, Northwestern University, Chicago, IL, USA.[34]Department of Biostatistics and Computational Biology, University of Rochester School of Medicine and Dentistry, Rochester, NY, USA. [35]Division of Rheumatology and Clinical Immunology, University of Pittsburgh School of Medicine, Pittsburgh, PA, USA. [36]Department of Biomedical Sciences, Humanitas University and Humanitas Research Hospital, Milan, Italy. [37]Division of Immunology and Rheumatology, Institute for Immunity, Transplantation and Infection, Stanford University School of Medicine, Stanford, CA, USA. [38]Department of Radiology, University of Pittsburgh Medical Center, Pittsburgh, PA, USA. [39]Rockefeller University, New York, NY 10065, USA.